# REGIONAL DEPTH-PHASE DETECTION AND FOCAL DEPTH ESTIMATION: APPLICATION TO EVENTS IN SOUTHEAST ASIA

Anastasia Stroujkova and Delaine Reiter

Weston Geophysical Corporation

Sponsored by National Nuclear Security Administration
Office of Nonproliferation Research and Development
Office of Defense Nuclear Nonproliferation

Contract No. DE-FG02-03ER83820

## ABSTRACT

The accurate estimation of the depth of small, regionally recorded events continues to be an important and difficult monitoring research problem. Our previous studies on detecting regional-distance depth phases using cepstral techniques have yielded only a moderate level of success. Therefore, we are investigating other waveform characteristics and detection techniques that can enhance the accuracy of regional focal depth estimation. In particular, we are combining enhanced signal processing in the complex *Pn* coda of regional seismograms, sparse-network hypocenter locations, and surface-wave inversions for depth and focal mechanism to determine an event's focal depth.

Our work during the preceding year was two-fold. First, we continued research into developing improved array-processing techniques for regional depth-phase detection. The cepstral F-statistic method that we have employed in the past (Bonner et al., 2002) cannot be used to reliably identify depth phases on its own. Other evidence must be used to help determine whether the phase in question is truly a depth phase. For example, apparent velocities, amplitudes and the frequency content of both the direct arrival and suspected surface reflections should be taken into consideration. We used a variety of array methods to estimate apparent phase velocities, including beam-forming, semblance analysis, MUltiple SIgnal Classification (MUSIC) (e.g., Capon, 1969; Schissele et al., 2004), and cross-correlation (e.g., Cansi, 1995; Tibuleac and Herrin, 1997). To facilitate the processing and comparison of results, we developed a MATLAB-based processing tool, which allows application of the various techniques in a single environment.

The second part of our research effort involved the comparison of different depth estimates obtained by both body- and surface-wave techniques. For example, we used a grid-search, multiple-event location method (Rodi, 2005) to estimate hypocenters from body-wave arrivals observed on sparse networks of regional stations. We studied the influence of different factors on the resulting focal depth estimate, such as the velocity model and network geometry. In addition, we applied surface-wave analysis, which can also be used to determine event focal mechanism (Herrmann, 2002), to our regional network data. The surface-wave analyses in turn can provide useful information on the relative amplitudes of the direct and surface reflected arrivals.

To validate our approach and provide quality control for our solutions, we applied the techniques to moderated-sized events ($m_b$ ~ 4.5-6.0) with independently determined focal mechanisms. In this paper we illustrate the techniques using regional events observed at the KSAR (Wonju, South Korea) teleseismic array and other nearby broadband three-component stations. Our results indicate that the techniques can produce excellent agreement between the various depth estimates. However, in some cases there remains great variability between different depth estimates. This variability (as expected) is strongly related to validity of the velocity model employed, and to a lesser extent the recording station coverage.

## OBJECTIVES

The accurate identification of regional seismic depth phases such as *pPn* and *sPn* is a formidable task. Depth phases are the primary tool that seismologists use to constrain the depth of a seismic event. When depth phases from an event are detected, an accurate source depth is easily found by using the delay times of the depth phases relative to the *P* wave and a velocity profile near the source. Some of the available techniques to determine source depth from depth-phase data include body-wave modeling (Saikia and Helmberger, 1997; Goldstein and Dodge, 1998), beam forming (Murphy et al., 1999; Woodgold, 1999), and relative-amplitude techniques (Pearce, 1977). In our previous studies, we have utilized the seismic cepstrum, which is defined as the Fourier transform of the log of the spectrum of a time domain signal (Bogert et al., 1963; Oppenheim and Schafer, 1975). The cepstrum is designed to detect the periodicity that occurs in the power spectrum when echoes are present in the original signal due to the interference of the direct (*P*) and depth (*pP* and/or *sP*) phases.

Reiter and Shumway (1999) formulated a cepstral F statistic for depth estimation problems using a classical approach to detecting a signal in a number of stationarily-correlated time series. The method attaches a statistical significance level to peaks in the beamed cepstra of seismic data caused by echoes in the signal. The results provided in Bonner et al. (2002) suggest that the cepstral F-statistic method (CFSM) is best applied at epicentral distances greater than 15°, where teleseismic *pP* and *sP* are the most commonly observed depth phases. However, the determination of depth at regional distances for small-to-intermediate sized crustal depth events remains an important, difficult and unsolved seismological problem.

To address this deficiency in regional depth estimation, we have developed three techniques to obtain regional focal depth estimates. These techniques include 'assisted' cepstral processing, sparse-network travel-time locations and surface-wave dispersion inversion. To demonstrate our techniques, we have applied them to moderate-sized events located within regional distances of the KSAR seismic array in South Korea. Only regional stations were used in the processing in order to mimic small events recorded by a limited number of regional stations.

## RESEARCH ACCOMPLISHED

### Enhanced Cepstral Processing: Application to KSAR Data

As we noted in the previous section, the CFSM (Bonner et al., 2002) cannot be used to reliably identify regional depth phases on its own. While pre-processing techniques such as wavelet denoising have shown some promise in improving cepstral estimates, additional evidence must be used to confirm whether a phase detected by the CFSM is truly a depth phase. For example, apparent velocities, amplitudes and the frequency content of both the direct arrival and suspected surface reflections should be taken into consideration. Therefore, to estimate apparent phase velocities and back azimuths of *Pn* coda arrivals we have tested a variety of array methods, including beam-forming, semblance analysis, MUltiple SIgnal Classification (MUSIC) (Capon, 1969; Schisselé et al., 2004), and cross-correlation (Cansi, 1995; Tibuleac and Herrin, 1997). To facilitate the array processing and comparison of results, we developed a MATLAB-based processing tool, which allows application of all of these techniques in a single environment. Optional pre-processing tools in our MATLAB Graphical User Interface (GUI) include glitch removal, Fourier filtering, and wavelet denoising. This useful new tool is proving to be very adaptable; for example, we are also using it to identify upper-mantle triplicated *P*-wave phases observed at far-regional distances.

To illustrate our depth phase identification techniques at regional distances, we applied them to well-located events observed at regional distances from the KSAR (Wonju, South Korea) teleseismic array and other nearby broadband three-component stations. Five of the events have known focal mechanisms from the Harvard Centroid Moment Tensor (CMT) catalog (Figure 1). Table 1 provides the parameters of the events used in this study, including the depth estimates from the International Seismic Centre (ISC), the Experimental International Data Center (EIDC), and Harvard catalogs.

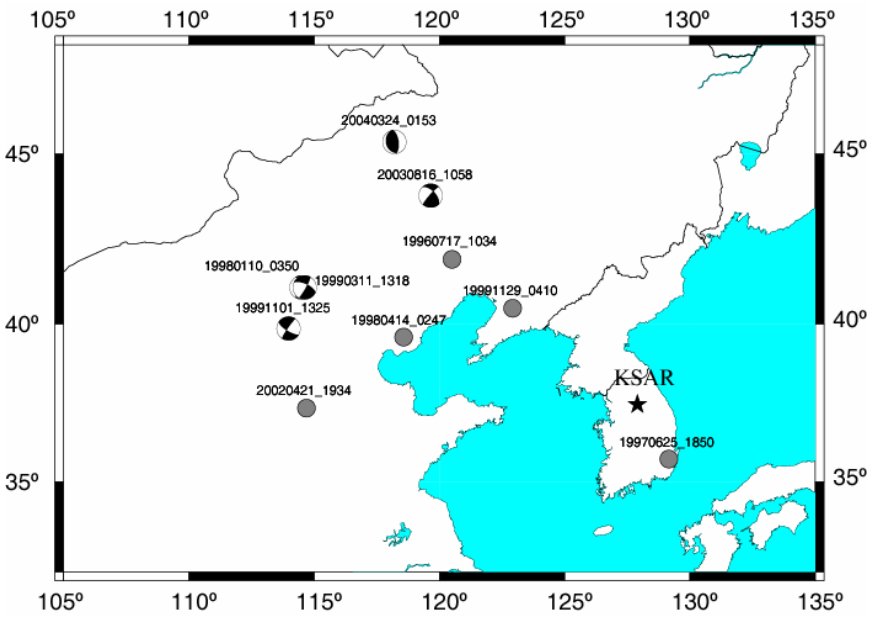


**Figure 1. Map showing the locations of study events. Focal mechanisms are shown for the events with available Harvard CMT solutions**

**Table 1. List of study events recorded at KSAR, with the ISC epicenter and the depths published by the ISC, EIDC and Harvard catalogs. Epicenter locations and magnitudes are given by ISC, with the exception of the event 20040324_0153 (EIDC).**

| Event Origin (ymmdd_hhmm) | Lat, ºN | Lon, ºE | Depth | | | $m_b$ |
|---|---|---|---|---|---|---|
| | | | ISC | EIDC | Harvard | |
| Events with Harvard CMT | | | | | | |
| 19980110_0350 | 41.14 | 114.52 | 16.7 | 4.8 | 15 | 5.3 |
| 19990311_1318 | 41.16 | 114.69 | 27 | 17 | 33 | 4.5 |
| 19991101_1325 | 39.91 | 114.05 | 0.0 | 10 | 15 | 4.7 |
| 20030816_1058 | 43.81 | 119.74 | 23.2 | 8.8 | 30 | 4.7 |
| 20040324_0153 | 45.38 | 118.15 | … | 18 | 13 | 5.4 |
| Other events | | | | | | |
| 19960717_1034 | 42.00 | 120.48 | 0.0 | 15.7 | … | 4.4 |
| 19970625_1850 | 35.75 | 129.17 | 13.5 | 13.5 | … | 4.2 |
| 19980414_0247 | 39.73 | 118.74 | 0.0 | 23.0 | … | 4.2 |
| 19991129_0410 | 40.39 | 122.95 | 38.6 | 10.0 | … | 4.5 |
| 20020421_1934 | 37.43 | 114.77 | 23.9 | 24.0 | … | 4.3 |

In previous work, Reiter et al. (2004) demonstrated the benefits of using wavelet denoising before applying the CFSM. Figure 2 shows the results from applying the CFSM with and without wavelet denoising to two of the events in Table 1. Both event records exhibit typical regional Pn with long codas and no clear depth phase candidate. Event 19991101_1325, shown in Figure 2a, has significant pre-event noise. After applying wavelet denoising in the 6$^{th}$-level decomposition, the pre-event noise is removed; however, the coda behavior doesn't change significantly (Figure 2b). The cepstral F-statistic of the wavelet-denoised

trace is almost identical to the one performed on the raw data; i.e., both results retain several false cepstral peaks.

Figures 2c and 2d show the results for Event 20020421_1934. For this example, the wavelet denoising at the 5th decomposition level removes a significant amount of *Pn* coda energy. The cepstral F-statistic also shows fewer false hits for the denoised data. The correct *pPn* arrival is one of the cepstral peaks, and it can be clearly identified on the seismic trace because of its similarity to the direct arrival. Note that both events appear to have complex source-time functions with more than one peak. In both cases the CFSM detected on the second peaks of the source-time functions, because they produce echoes similar to surface reflections.

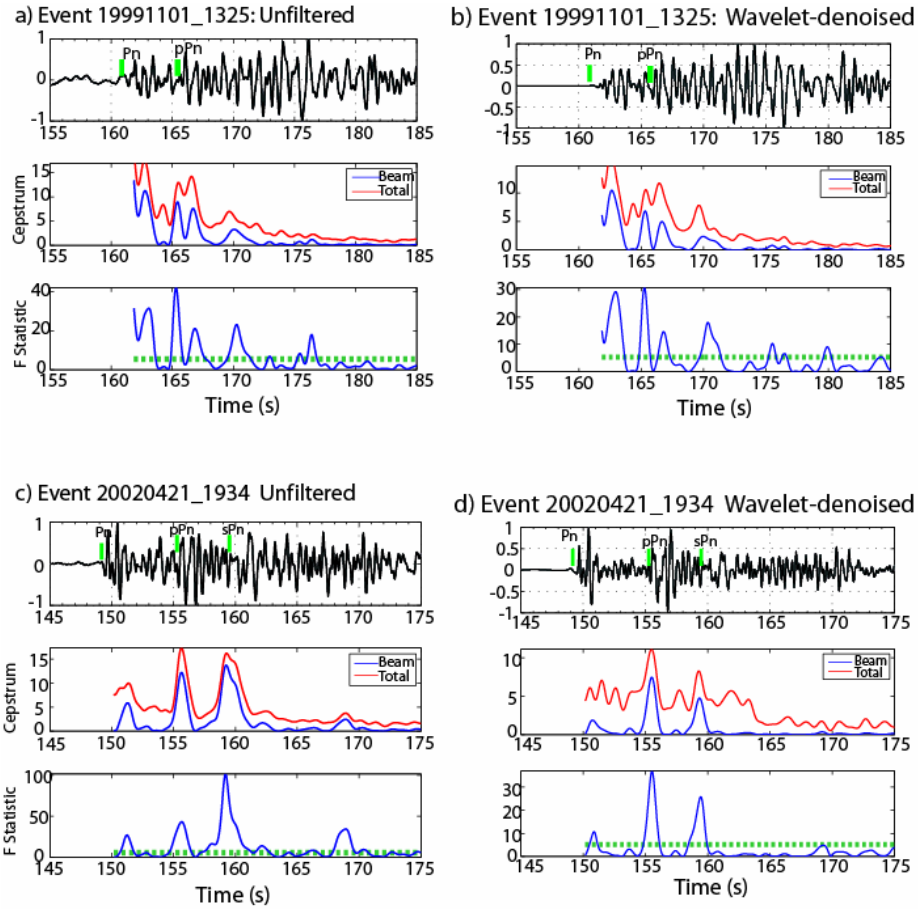


**Figure 2. Application of the CFSM to KSAR events before and after wavelet denoising. Each subpanel shows the array beam (top), the beam and total cepstra (middle plot), and the cepstral F-statistic with a green dashed 99% significance level (bottom). a) Event 19991101_1325 using unfiltered data; b) Event 19991101_1325 with wavelet denoising applied at decomposition level 6; c) Event 20020421_1934 using unfiltered data; d) Event 20020421_1934 with wavelet denoising at decomposition level 5.**

To help confirm cepstral detections of regional depth-phase arrivals, we apply a version of the MUSIC estimator (Schisselé et al., 2004), which utilizes a continuous wavelet transform (CWT) to help identify the time windows in which coherent phases exist. Once the user has defined a processing window, the MUSIC estimator calculates the propagation characteristics of the analyzed phase. In Figure 3 we show the results of applying the MUSIC estimator algorithm to the KSAR data for the two events analyzed in Figure 2. Figure 3a shows the estimator applied to both the *Pn* arrival (the time-frequency window is denoted by a horizontal white line in the CWT subplot) and to our candidate *pPn* arrival.

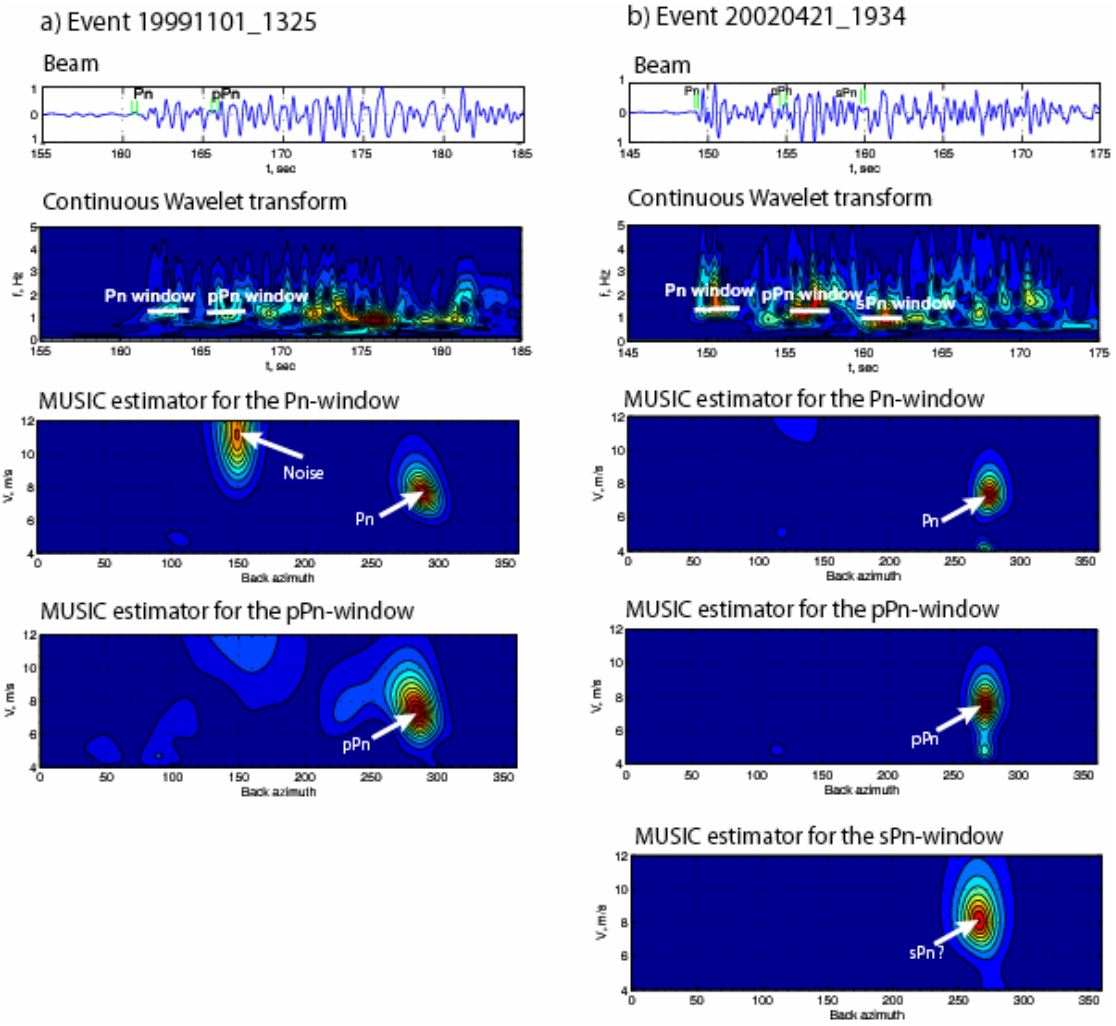


**Figure 3. MUSIC estimator analysis of the direct *Pn* and candidate depth phases for a) Event 19991101_1325 and b) Event 20020421_1934.**

As Figure 2 demonstrates, in most cases the CFSM produces more than one significant peak corresponding to suspected depth phases. To select the best depth phase candidates, we compute propagation parameters for the first arrival and for all other arrivals with a peak in the F-statistics, as shown in Figure 3. The secondary arrivals with the highest degree of similarity are selected as the best depth-phase candidates. Using this approach we estimated cepstra for the ten events in Table 1, and then found event depths by matching (*pPn-Pn*) travel time differences computed with the one-dimensional (1-D) *IASPEI91* reference model (Kennett and Engdahl, 1991). Table 2 shows the results of this analysis and compares the depth estimates derived from primary phases only to those that include the depth-phase arrival picks.

**Sparse-Network Regional Location and Focal Depth Estimates Using a Grid-Search Algorithm**

For the second depth estimation technique, we computed event hypocenters from a sparse network of regional observations using a Grid-search Multiple-Event Location algorithm (GMEL), which was initially developed at the Massachusetts Institute of Technology (Rodi and Toksöz, 2000; 2001). The algorithm employs a recursive grid-search technique to find the best-fitting location parameters (origin time and hypocenter) of an event, and a Monte Carlo method to determine confidence regions on the location parameters.

Routine network location procedures do not include regional depth-phase arrivals, which can lead to large uncertainties on the depths of small events observed only at regional distances. Reiter et al. (2002) demonstrated that the addition of regional depth-phase arrivals to the primary *Pn* arrivals in a sparse-network location procedure results in significantly better confidence on the depth estimate. Thus, we examined the effect of including CFSM-estimated *pPn* and *sPn* arrival times at KSAR in the GMEL relocation exercise. To supplement these travel-time picks, we included MUSIC-derived depth-phase candidate arrivals at some of the other regional three-component broadband stations. We also used available catalog *Pn* and *Sn* arrival picks for the regional stations located within 12º from each event. Figure 4 shows a comparison between confidence regions obtained with and without regional depth-phase travel times (Figures 4a and 4b, respectively). Adding correctly identified regional depth-phase picks to the location procedure significantly constrains the depth in the confidence regions.

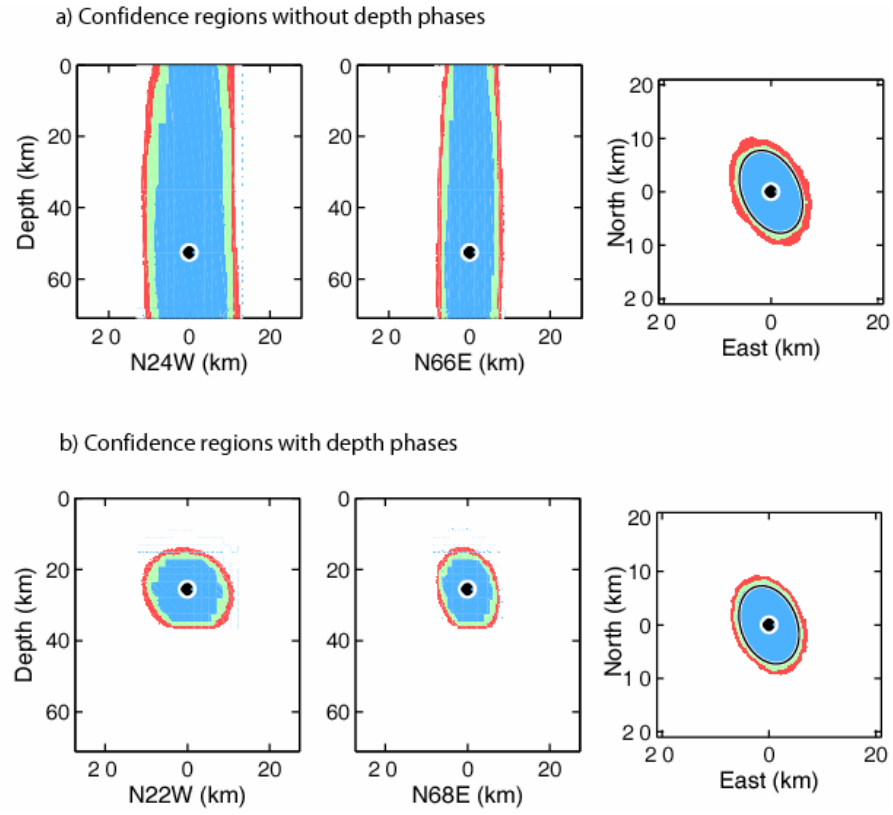


**Figure 4. GMEL location confidence intervals for Event 20020421_1934. Each panel shows the depth confidence regions (above 95%) in the left and middle subplots and the epicentral confidence region in the right subplot. The black dot shows the best-fitting hypocenter. a) sparse-network location performed without additional regional depth-phase picks; b) sparse-network location performed with regional depth-phase picks. The results in b) demonstrate improved depth constraints.**

Table 2 summarizes the results of depth estimates for the 10 events shown in Table 1. The results indicate that there is a reasonably good agreement between the inversion results and the depths estimated directly from cepstra.

### Depth Estimates and Focal Mechanisms from Surface-Wave Inversions

Regional surface-wave observations present another source of data that we can use to estimate both event depth and focal mechanism. Tsai and Aki (1970) and Douglas et al. (1971) demonstrated that Rayleigh

waves can produce notches in the amplitude spectrum. The frequency at which these notches occur is dependent on both the hypocenter depth and the observed azimuth from the event epicenter to the station. This approach has been used successfully by other researchers such as Nguyen and Herrmann (1992) and Patton (1998).

In this study we used the source inversion codes written by Dr. Robert Herrmann of St. Louis University. He has developed and published programs to invert the spectral amplitudes of Rayleigh and Love waves in his Computer Programs in Seismology software package (Herrmann and Ammon, 2002). We used Herrmann's program *srfgrd96* (aka *surf96*), which is a grid-search inversion technique that determines the combination of moment, depth and focal mechanism that minimizes the misfit between observed and predicted surface-wave amplitude spectra. The input required for the inversion consists of the amplitudes of the fundamental Rayleigh and Love waves and a 1-D regional Earth model. The program searches over a model space of moment $M_0$, depth h, strike $\phi$, dip $\delta$, and rake $\lambda$ to find best-fitting solutions based on the observed amplitude spectra.

We applied *srfgrd96* to the 10 events listed in Table 1. To pick surface wave dispersion curves we used 3-component broadband data from stations located at regional distances from the events. As before, we performed the inversion using the *IASPEI91* reference model; Table 2 includes these results in the column marked '*surf96'*. In general the agreement between the depth estimates contained in the three right-hand columns is quite good.

**Table 2. Depth estimates for the events in Table 1 using the three techniques discussed in the paper. Numbers in brackets show numbers of data points used for the event location (number of phase travel times for GMEL and number of stations for which dispersion curves were measured).**

| Event | Depth (EIDC bulletin) | Depth (km) estimated with *IASPEI91* | | | |
|---|---|---|---|---|---|
| | | GMEL: no pPn (# of phases) | GMEL: with pPn (# of phases) | *surf96* (# of stations) | Cepstrum |
| Events with Harvard CMT | | | | | |
| 19980110_0350 | 4.8 | 35.0 (16) | 12.0 (19) | 14 (4) | 14.2 |
| 19990311_1318 | 17 | 0.0 (24) | 10.9 (28) | 9 (7) | 9.7 |
| 19991101_1325 | 10 | 18.2 (16) | 17.9 (20) | 17 (6) | 19.2 |
| 20030816_1058 | 8.8 | 35.0 (22) | 19.1 (24) | 13 (5) | 16 |
| 20040324_0153 | 18 | 0.0 (14) | 15.0 (17) | 9 (5) | 19 |
| Other events | | | | | |
| 19960717_1034 | 15.7 | 0.0 (8) | 16.3 (10) | 5 (3) | 8.9 |
| 19970625_1850 | 13.5 | 2.8 (29) | 11.6 (32) | 13 (5) | 11.4 |
| 19980414_0247 | 23.0 | 35.0 (13) | 3.7 (16) | 8 (7) | 9.7 |
| 19991129_0410 | 10.0 | 0.01 (15) | 9.7 (18) | 11 (3) | 13.8 |
| 20020421_1934 | 24.0 | 52.6 (20) | 26.4 (24) | 21 (3) | 27.3 |

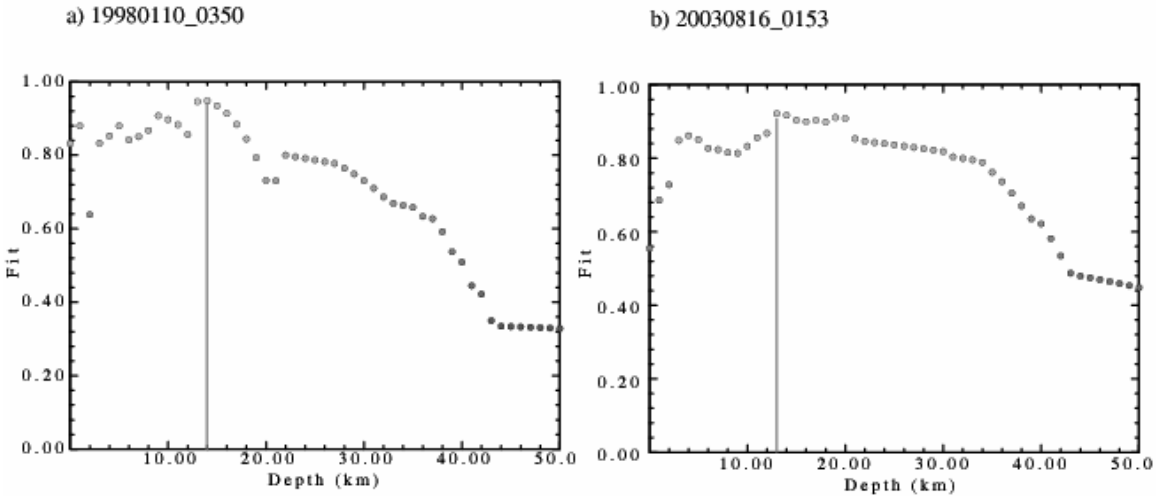


**Figure 5. Confidence levels calculated by the surface-wave amplitude inversion routine *srfgrd96* for a) Event 19980110_0350 and b) Event 20030816_1058. Vertical lines show the estimated depth of the event.**

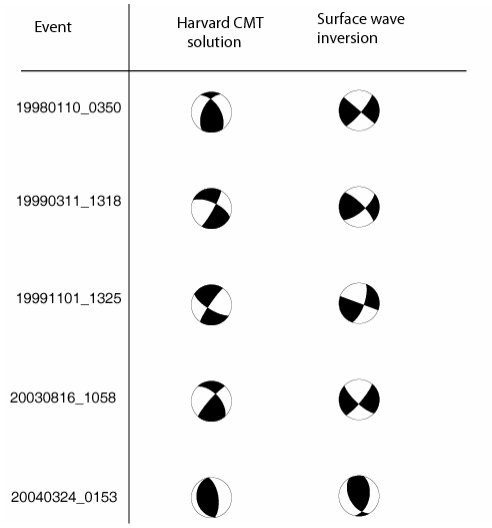


**Figure 6. Comparison of the Harvard CMT catalog solutions for events in Table 1 with the ones determined by surface-wave inversion of the regional data.**

In Figure 5 we show two examples of the fit in depth estimated by the surface-wave amplitude inversion routine. Figure 6 shows the focal plane solutions computed from the regional station data compared to the Harvard CMT solutions for the relevant events in Table 1. Four out of five focal-plane solutions are in good agreement with the Harvard catalog. Only one event (19980110_0350) resulted in a poor match, even though the surface-wave depth estimate is in good agreement with the cepstral and network location depth estimates. This mismatch in focal solution is likely caused by the small number of stations used in the inversion procedure (4, as indicated in Table 2).

## CONCLUSIONS AND RECOMMENDATIONS

We continue to study the problem of determining accurate focal depths for regionally-recorded (small) events. In this paper we combined and compared three different techniques to obtain estimates of focal depths for earthquakes. These techniques included enhanced cepstral processing, in which we supplement cepstral detections of regional phases with additional information such as the phase velocities and back azimuths of candidate phases. This additional information aids in the accurate identification of a depth-phase arrival, which can then be directly inverted for depth or used as a constraint in our second depth-estimation technique: regional network travel-time locations. The third method we have tested is the inversion of surface-wave amplitudes for focal depths and mechanisms using regional station data. While this method shows some promise, it is hampered by its sensitivity to the velocity model used and the requirement for many stations to provide solution stability. However, we may be able to use the surface-wave inversions to confirm or eliminate depths calculated by enhanced cepstral processing and network travel-time locations

We have applied our techniques to data from several seismic arrays in Asia and reported in this paper on results from the KSAR array in South Korea. With this array event depths estimated using depth-phase information show better consistency and lower sensitivity to the velocity model, but this is not always the case.

Our future focus will be to statistically combine the estimates from the different techniques to provide quantitative confidence levels on regional focal depths derived using multiple methods. In addition, we will continue to develop and test additional methodologies to improve the accurate detection of regional depth phases and estimates of event focal depth.

## REFERENCES

Bogert, B. P., M. J. R. Healy and J. W. Tukey (1963). The quefrency analysis of time series for echoes: cepstrum, pseudo-autocovariance, cross-cepstrum and saphe cracking, in *Proceedings of a Symposium on Time Series Analysis*, ed. M. Rosenblatt, John Wiley and Sons, Inc., New York.

Bonner, J. L, D. T. Reiter, and R. H. Shumway (2002). Application of a cepstral F statistic for improved depth estimation, *Bull. Seism. Soc. Am* 92: 1675–1693.

Cansi, Y. (1995). Earthquake location applied to a mini-array: K-spectrum versus correlation method, *Geophys. Res. Lett.* 20: (17), 1819–1822.

Capon, J. (1969). High-resolution frequency-wavenumber spectrum analysis, *Proc. of the IEEE*, 57: p. 1408–1418.

Douglas, A., J. A. Hudson and V. K. Kembhavi (1971). The relative excitation of seismic surface and body waves by point sources, *Geophys. J. R. Astr. Soc*. 23: 451–460.

Goldstein, P., and D. Dodge (1998). Depth and mechanism estimation using waveform modeling, in *Proceedings of the 20th Annual Seismic Research Symposium on Monitoring a Comprehensive Test Ban Treaty (CTBT)*, pp. 238–247.

Herrmann, R., and C. Ammon (2002). Surface waves, receiver functions and crustal structure, in *Computer programs in seismolo*gy.

Herrmann, R., Y.-S. Jeon, W. Walter, and M. Pasyanos (2005). Seismic source and path calibration in the Korean Peninsula, Yellow Sea and Northeast China, in *Proceedings of the 27th Seismic Research Review: Ground-Based Nuclear Explosion Monitoring Technologies,* LA-UR-05-6407, Vol. 1, pp. 42–51.

Kennett B. L. N., and E. R. Engdahl (1991). Travel times for global earthquake location and phase identification, *Geophys. J. Int.* 105: 429–465.

Melton, R. S., and L. F. Bailey (1957). Multiple signal correlators, *Geophys.* 22: 565–588.

Murphy, J. R., R. W. Cook, and W. L. Rodi (1999). Improved focal depth determination for use in CTBT monitoring, in *Proceedings of the 21st Seismic Research Symposium: Technologies for Monitoring the Comprehensive Nuclear-Test Ban Treaty,* LA-UR-99-4700, Vol. 1, 50–55.

Nguyen, B. V., and R. B. Herrmann (1992). Determination of source parameters for central and eastern North American earthquakes (1982-1986), *Seism. Res. Lett.* 63**:** 567–586.

Oppenheim, A. V., and R. W. Schafer (1975). *Digital Signal Processing*, Prentice Hall, New York.

Patton, H. J. (1998). Bias in the centroid moment tensor for central Asian earthquakes: evidence from regional surface wave data, *J. Geophys. Res*. 103: 26963–26974.

Pearce, R. G. (1977). Fault plane solutions using relative amplitudes of *P* and *pP*, *Geophys. J. R. Astr. Soc*. 50: 381–394.

Reiter, D. T., and R. H. Shumway (1999). Improved seismic event depth estimate using cepstral analysis, in *Proceedings of the 21st Seismic Research Symposium: Technologies for Monitoring the Comprehensive Nuclear-Test Ban Treaty*, LA-UR-99-4700, Vol. 1, pp. 599–606.

Reiter, D. T., J. L. Bonner, C. E. Vincent and J. Britton (2002). Incorporating secondary phases in 3-D regional seismic event location: application to the sparse network problem, in *Proceedings of the 24th Seismic Research Review—Nuclear Explosion Monitoring: Innovation and Integration,* LA-UR-02-5048, Vol. 1, pp. 375–384.

Reiter, D., A. Rosca, H. Hooper, J. Bonner, C. Vincent and W. Rodi (2003). Improved regional seismic event location using 3-D velocity models, Final Report, Contract DTRA01-00-C-0098.

Reiter, D. T., J. L. Bonner, and R. Shumway (2004). Development of innovative filtering techniques for improved depth phase detection at regional distances, in *Proceedings of the 26th Seismic Research Review: Trends in Nuclear Explosion Monitoring,* LA-UR-04-5801, Vol. 1, pp. 287–296.

Rodi, W. (2005). The grid-search multiple event location (GMEL) algorithm reference manual (rodi@erl.mit.edu), Massachusetts Institute of Technology.

Rodi, W. and M. N. Toksöz (2000), Grid-search techniques for seismic event location, in *Proceedings of the 22nd Annual DoD/DOE Seismic Research Symposium*: *Planning for Verification of and Compliance with the Comprehensive Nuclear-Test-Ban Treaty (CTBT)*, Vol. 2, pp. 339–348.

Rodi, W., and M. N. Toksöz (2001). Uncertainty analysis in seismic event location, in *Proceedings of the 23rd Seismic Research Review: Worldwide Monitoring of Nuclear Explosions,* LA-UR-01-4454, Vol. 1, pp. 324–332.

Saikia, C. K. and D. V. Helmberger (1997). Approximation of rupture directivity in regional phases using upgoing and downgoing wave fields, *Bull. Seism. Soc. Am.* 87: 987–998.

Schisselé, E., J. Guilbert, S. Gaffet, and Y. Cansi (2004). Accurate time–frequency–wavenumber analysis to study coda waves, *Geophys. J. Intl.* 158: (2), 577–591.

Shumway, R. H., S. E. Kim, and R. R. Blandford (1999). Nonlinear estimation for time series observed on arrays, Chapter 7, S. Ghosh ed., *Asymptotics, Nonparameterics and Time Series*, New York: Marcel Dekker.

Tibuleac, I. M. and Herrin, E, (1997), Calibration Studies at TXAR, *Seismological Res. Lett.* 68: 353–365.

Tsai, Y. B., and K. Aki (1970), Precise focal depth determination from amplitude spectra of surface waves, *J. Geophys. Res*. 75: 5729–5743.

Woodgold, C. R. D. (1999), Wide-aperture beamforming of depth phases by timescale contraction, *Bull. Seis. Soc. Am*. 89: 165–177.